Electrical and Optical Properties of Fullerenol Langmuir−Blodgett Films Deposited on Polyaniline Substrates

ARTICLE *in* THE JOURNAL OF PHYSICAL CHEMISTRY B · APRIL 2003

Impact Factor: 3.3 · DOI: 10.1021/jp022159z

4 AUTHORS, INCLUDING:

Marina Rincón
Universidad Nacional Autónoma de México
94 PUBLICATIONS **1,320** CITATIONS
SEE PROFILE

Jose Campos
Universidad Nacional Autónoma de México
47 PUBLICATIONS **963** CITATIONS
SEE PROFILE

Jaime Ruiz-Garcia
Universidad Autónoma de San Luis Potosí
65 PUBLICATIONS **983** CITATIONS
SEE PROFILE

Electrical and Optical Properties of Fullerenol Langmuir−Blodgett Films Deposited on Polyaniline Substrates

M. E. Rincón,*,† H. Hu,† J. Campos,† and J. Ruiz-García‡

Centro de Investigación en Energía−UNAM, Apartado Postal 34, Temixco, Mor. 62580, Mexico, and Instituto de Física−UASLP, Álvaro Obregón 64, San Luis Potosí, SLP 78000, Mexico

Received: September 26, 2002; In Final Form: January 31, 2003

The synthesis of fullerenol with various degrees of hydroxylation and the use of a low hydroxylated product to form stable Langmuir films are reported in this work, along with the optical and electrical properties of Langmuir−Blodgett (LB) films obtained on glass and polyaniline (PANI) substrates. The data suggest that an average of 9−12 hydroxyl groups are bound preferentially on one side of the C_{60} cage and this allows the formation of stable two-layer films at the air/water interface. The large anisotropy of the hydroxylated molecule provides organized LB films of the type *substrate−(D−C*$_{60}$*−D−C*$_{60}$*−)*$_n$, with D representing the hydroxyl groups. The electrical conductivity of LB films deposited on glass is equivalent to that reported for highly conductive polymeric C_{60} but several orders of magnitude higher than that for disordered fullerenol pellets. UV−vis absorptions provide evidence that fullerenol layers cause the deprotonation of PANI, rendering a polymer with low conductivity. The loss of conductivity disagrees with the behavior expected for a donor (PANI)/acceptor (fullerenol) interface, even though current−voltage ($I-V$) curves of fullerenol$_{LB}$/PANI junctions indicate some degree of electrical rectification. Additionally, transients observed at large bias on the $I-V$ curves agree with the reported proton conductivity of fullerenol.

Introduction

The chemistry of fullerene C_{60} and its derivatives has attracted a great deal of interest due to the outstanding physical and chemical properties of these compounds. Among the great number of derivatives that have been synthesized, water-soluble fullerene derivatives have been investigated to date mostly within the framework of biological and medical applications.[1−3] Fullerenol, synthesized for the first time by Chiang et al.,[4−9] is a good example of a water-soluble fullerene derivative; however, this compound has been used not only in medical applications[10−17] but also as a piezoelectric[18] and proton conducting material.[19]

Our research interest in these compounds is based upon their potential use as new materials for solar energy conversion and storage. These applications of fullerenes have attracted much interest since the discovery of photoinduced electron-transfer processes in composites of conductive polymers and C_{60}.[20] Since then, most of the research efforts have been focused on understanding the optoelectronic properties of the donor/acceptor interface and developing new ways to avoid bulk recombination of the photogenerated carriers. Currently, it is well accepted that the design of new composites based on polymers and fullerene derivatives, particularly the choice of heterojunction, will be limited by our ability to impose some structural ordering through miscibility control of the various phases.

Recently, we have found that deposition of commercial fullerenol (Aldrich: $C_{60}(OH)_{24-28}$) (unpublished results) by the method of drop and evaporation produces discontinuous and disordered films on glass substrates. The disordered film degrades the electrical properties of polymeric substrates, such as polyaniline (emeraldine salt) and polypyrrole, by several orders of magnitude. This raises the interesting possibility that the electrical properties of the conductive polymer/fullerenol junction can be improved by reducing the number of hydroxyl groups and by attempting highly organized structures at the interface.

The conductive properties of fullerenol have been reported to be more ionic than electronic and a function of the amount of hydroxyl groups.[19] Highly hydroxylated molecules typically are associated with a dielectric material, while low levels of hydroxylation indicate a proton conductive material with ionic conductivity of $7 \times 10^{-6}\ \Omega^{-1}\ cm^{-1}$. Although extensive work on the formation of Langmuir and Langmuir−Blodgett films has been reported recently on several fullerene derivatives,[21,22] the formation of monolayers at the air/water interface has been difficult to achieve due to the high water solubility of the fullerenols. The work of Chiang et al.[9,23] indicates that fullerenol water solubility depends on the number of OH's attached to C_{60}. These authors were able to obtain Langmuir films of $C_{60}(OH)_{12}$ and reported a minimum area per molecule of 190 Å^2. The thickness of a two-layer $C_{60}(OH)_{12}$ LB film deposited on mica was measured to be 13 Å/layer (approximately the diameter of a molecule), supporting their evidence of monolayer formation at the air/water interface.[23]

In this work we also attempted monolayer formation of fullerenol. To do so, we modified the synthesis of highly soluble fullerenol to obtain different degrees of hydroxylation and used the water-insoluble fraction to form LB films on various substrates. IR analysis and MALDI-MS experiments were run to identify the approximate number of hydroxyl groups in the selected fraction, while UV−vis spectroscopy and electrical characterization studies gave information on the LB films deposited on glass and on polyaniline substrates. For pur-

* Corresponding author. E-mail: merg@cie.unam.mx.
† Centro de Investigación en Energía−UNAM.
‡ Instituto de Física−UASLP.

10.1021/jp022159z CCC: $25.00
Published on Web 04/08/2003

TABLE 1: Reactants and Products of the Various Hydroxylation Reactions

	I	II	III	IV
C_{60} (g)	0.5	0.5	0.5	0.5
o-DCB (mL)	50	10	10	10
TBACl (mg)	150	30	30	30
Na_2O_2 (g)	6.9	1.5	0.5	0.5
30% H_2O_2 (mL)			15	15
H_2O (mL)	50	10		
temp (°C)/time	80/17 h	80/10 min	25/10 min	25/10 min
$Na_2S_2O_3$ (g)				0.25
product soluble in water	O17	80-10-L		~10%
product insoluble in water	~0%	80-10	25-10-1	25-10-Ta
			25-10-2	25-10-Tb

poses of comparison and control, LB films of a less hydrophilic compound, a substituted fulleropyrrolidine derivative ($C_{60}CH_2NCH_3CHC_6H_5$; MW = 853), were also formed and subjected to the same characterization.

Experimental Section

Synthesis of $C_{60}(OH)_n$, $n = 1-16$. Various fullerenols were synthesized from the corresponding fullerenes by a procedure similar to that used by Li et al.[24] A mixture of solutions consisting of 1 g of C_{60} dissolved in 100 mL of *o*-dichlorobencene (*o*-DCB), and 300 mg of tetrabutylammonium chloride hydrate and 13.8 g of sodium peroxide (Na_2O_2) dissolved in 100 mL of water was stirred at 80 °C for 24 h. After the reaction, the organic phase *o*-DCB became colorless and was separated from the aqueous phase by a separatory funnel. The dark brown aqueous mixture was poured into 400 mL of methanol and centrifuged. The solid thus obtained was washed several times with methanol and dried in a vacuum oven. The dried solid was dissolved in a minimum amount of water and neutralized with aqueous HCl solution followed by neutralization by passing the solution through Amberlyst 15 ion-exchange resin using diluted aqueous HCl solution as eluent. The eluted aqueous solution was lyophilized over a period of several days. A dried light brown solid, soluble in THF, EtOH, and water, was obtained. As a major difference from the commercial fullerenol, the compound obtained by this method still fluoresces, giving an indication that the number of hydroxyl groups attached to the fullerene molecule is much lower than 24−28.

To decrease the number of hydroxyl groups in the C_{60} cage, variations of the reaction time, temperature, oxidant agent, and ratio of C_{60}/oxidant agent were attempted (Table 1 provides the details of each run). The yield of these reactions was very low, since two-phase catalysis is aimed to obtain highly hydroxylated fullerenes (i.e., the inorganic, water-soluble oxidant acts preferentially in the fullerene molecules that get into the aqueous phase after addition of few hydroxyl groups). The separation and purification of the various water-insoluble fractions were performed by solubility differences in solvents of differing polarity, followed by thin-layer chromatography (E. Merck: Analytical Plastic Backed Plates/Silica Gel 60 F254; developing solvent, methanol).

FTIR and MALDI-MS. The different fractions were characterized by FTIR and mass spectrometry analysis. FTIR measurements were performed on a Nicolet infrared spectrophotometer in the diffuse reflectance mode (DRIFT). The spectra were recorded at a resolution of 4 cm^{-1} and averaged over 64 scans. The mass spectrometry studies were carried out using the matrix-assisted laser desorption ionization (MALDI) technique, with either 2,5-dihydroxybenzoic acid (DHB), 9-nitroanthracene (NA), or anthracene (A) as matrix material.

Monolayer and LB Films: Formation and Characterization. The first step in the preparation of monolayers involved preparing several fractions that were allowed to sit overnight in small beakers filled with water. The fractions were dissolved in appropriate solvents, and a drop was carefully deposited on top of the water surface. The evolution of the meniscus formed between the water and the added solution was monitored overnight. In the majority of the fractions, the meniscus either disappears (fullerenol dissolves in water) or forms lenses close to the beaker wall. Only one water-insoluble but methanol-soluble fraction had kept the meniscus overnight. This fraction was the most hydroxylated product that was still insoluble in water. From this fraction, labeled 80-10, 2.6 mg was dissolved in a minimum amount of DMSO (2 mL) and then diluted with chloroform up to a 25 mL final volume. The working solution had an approximate concentration of 0.052 mg/mL (6×10^{-5} M; 3.5×10^{13} molecules/μL). For the substituted fulleropyrrolidine derivative, 2.1 mg was dissolved in 25 mL of chloroform. This gave a working solution with 0.084 mg/mL (10^{-4} M; 6×10^{13} molecules/μL).

Aliquots of the working solution were carefully spread onto a deionized water subphase (Millipore Milli-Q, resistivity 18 MΩ cm) in a vibration-isolated Lauda film balance at room temperature. The spread solutions were left for periods ranging from 20 min to 1 h, after which they were compressed at a barrier speed of 20 mm/min. The monolayer film at the air/water interface was transferred by the vertical transfer method (X-configuration) onto semiconducting polyaniline films deposited on conducting glass substrates (PANI/ITO), and also on pretreated Corning Glass slides. The glass slides were pretreated in the following manner: they were cleaned with $CHCl_3$, dried for 5 min in an oven, immersed for 1 day in a 1:1 H_2SO_4/H_2O 30% by weight solution prepared with Millipore water, and rinsed with Millipore water two or three times before clamping.

Results and Discussion

Synthesis of $C_{60}(OH)_n$, $n = 1-16$. In the aqueous phase, the reaction of Na_2O_2 with water produces a basic medium and peroxides as the strongest oxidant agent ($Na_2O_2 + H_2O \rightarrow HOO^- + OH^- + 2Na^+$). It is expected that the reaction starts when the phase-transfer catalyst transfers the nucleophile (HOO^-) as an ion-pair into the organic phase. In the organic phase the peroxide reacts with fullerene, opening the double bond and forming an epoxide:

$$C{=}C + {}^-O{-}O{-}H \rightarrow \text{epoxide} + OH^-$$

The opening of the ring is catalyzed by the basic medium, resulting in fullerene salt as the main product before hydration or acidification:

$$^-O{-}C{-}C{-}OH + H_2O \text{ or } HCl \rightarrow HO{-}C{-}C{-}OH + OH^- \text{ or } Cl^-$$

Under the reaction conditions described in Table 1, the final products were (a) highly hydroxylated fullerene, extremely soluble in water and in organic polar solvents, fractions labeled A24, O17, and 80-10-L; and (b) fullerene with medium hydroxylation, insoluble in water but soluble in methanol, fractions labeled 80-10, 25-10-1, and 25-10-Ta; and (c) fullerene with low hydroxylation, insoluble in water and methanol, soluble in nonpolar solvents, fractions labeled 25-10-2 and 25-10-Tb.

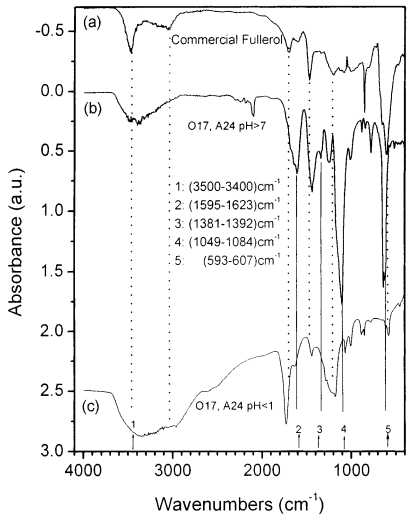

Figure 1. FTIR spectra of the different fractions obtained under the reaction conditions described in Table 1: (a) commercial product; (b) water-soluble fractions before ion exchange; (c) water-soluble fractions after ion exchange.

FTIR and MALDI-MS Characterization. The degree of hydroxylation was inferred from the FTIR spectra (Figure 1) of the different fractions, by monitoring the relative intensities of the peaks assigned to fullerenol {3430 (br, OH), 1631−1595 (br, C═C), 1392−1385 (br), 1090−1070 (br, C−O), 593−450 (br) cm^{-1}} and to fullerene {strong and narrow absorption peaks at 526, 576, 1182, and 1428 cm^{-1}}. In the IR spectrum of the commercial product (Figure 1a), the bands at 3467, 1603, 1079, and 606 cm^{-1} could be attributed to the absorption of fullerenol, although the 1392 cm^{-1} band is absent. The presence of other absorption bands (3042, 1692, 1240 cm^{-1}) has been reported for fullerenol prepared from alkaline synthesis, whenever the reaction product is treated with an acidic ion exchanger.[24] These bands have also been observed in the product obtained from the reaction of C_{60} with strong acids, but only when the reaction product has been subjected to further acidic treatment.[6] Their origin has been explained in terms of the catalyzed conversion of vicinal hydroxy groups to the corresponding ketone structure,[24] or by the presence of hemiketals in the structure of fullerenols derived from aqueous acid chemistry.[6]

In our synthesis, the IR spectra (Figure 1b) of the water-soluble fractions taken before ion exchange (Na-form) also show absorptions due to fullerenol (3397, 1607, 1340, 1104, ∼620 cm^{-1}). Still, the shoulder around 1680 cm^{-1}, together with medium broad bands centered at 1436 and 1244 cm^{-1}, suggests the presence of carbonyl groups, phenolic groups, or dioxygenated carbons (hemiketal or lactone structures).[25] After ion exchange, the IR spectrum (Figure 1c) of the vacuum-dried sample obtained after lyophilizing the eluted fraction shows the conversion reported by Li et al. (i.e., new absorptions due to ketone groups at 1732 and 1283 cm^{-1}).[24]

The evolution of the hydroxylation reaction is shown in Figure 2 from top to bottom. Here, the FTIR spectra correspond to the water-insoluble products. The first spectrum (Figure 2a) shows the reactant C_{60}, while the second (Figure 2b) belongs to the fraction 25-10-T, which is obtained when the reaction is terminated by addition of thiosulfate and takes place at room temperature over a period of 10 min. At this stage, very little hydroxylation has been achieved, although the increase in relative intensity of absorption bands at 1035 and 749 cm^{-1} suggests that fullerene modification is already taking place. In the third spectrum (Figure 2c), the appearance of bands at 3486

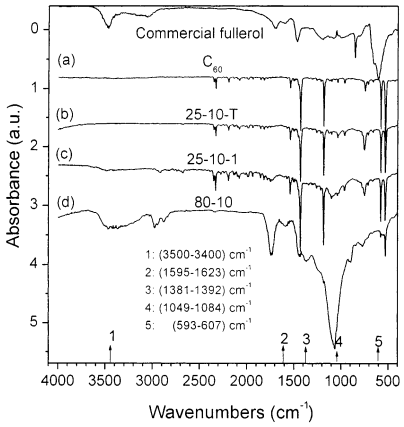

Figure 2. FTIR spectra showing the evolution of the hydroxylation reaction: (a) reactant C_{60}; (b) fraction 25-10-T (reaction took place at room temperature during 10 min and was terminated by addition of thiosulfate); (c) fraction 25-10-1 (10 min reaction at 25 °C); (d) fraction 80-10 (10 min reaction at 80 °C). In parts c and d the reaction was terminated by suspending the stirring and allowing the organic and aqueous phases to separate.

and 1099 cm^{-1} indicates the formation of fullerenol. The spectrum belongs to the fraction obtained from the reaction run at room temperature during 10 min under vigorous stirring. The reaction stops once the stirring is suspended and the phases separate. If the reaction takes place at 80 °C during 10 min (product labeled 80-10), the bands of fullerenol are better defined (Figure 2d). The spectrum shows absorption bands of fullerenol at 3466, 1584, 1366, and 1062 cm.$^{-1}$ The absorption bands at 1741, ∼1180, and 897 cm^{-1} can be related to the vibrations of carbon−oxygen bonds (ring ketones, aryl ethers, peroxides), suggesting incomplete hydroxylation (i.e, fullerenol salts instead of fullerenol) and/or the opening of the cage during the first steps of hydroxylation under alkaline conditions. This fraction was used to form monolayers, and no attempt was made to separate the effects due to the presence of incomplete hydroxylated product.

The process of hydroxylation was also followed qualitatively by mass spectrometry studies. Here, the clear dependency of the fragmentation pattern with laser fluency suggests the enrichment of the fraction with small n at the expense of the degradation of highly hydroxylated fractions. As a reference, the commercial fullerenol, labeled as $C_{60}(OH)_n$, with $n = 24-28$, has a fragmentation pattern that ends at $n = 7$ in the DHB matrix. Similarly, different matrixes gave different degrees of hydroxylation. Regardless of these differences, the classification of the different fractions according to the degree of hydroxylation (Table 2) is the same in both the DBH and NA matrixes, while the A matrix does not give any meaningful information. Table 2 also classifies the various fractions according to the results of TLC and FTIR, giving additional information about the polarity of the different fractions. All of these synthesized fullerenols are mixtures that are difficult to separate, especially if the synthesis is forced to stop at a low degree of hydroxylation, when much of the product is still in the organic phase. The results of thin-layer chromatography indicated that the fractions obtained were mixtures and that our attempts to separate the different fractions using a spectrum of solvents with different polarity had just a moderate degree of success.

Monolayer Formation. As indicated above, the fraction labeled 80-10 was used in the formation of Langmuir films because it was the product with the highest number of hydroxyl groups that was still insoluble in water. From Table 2 and Figure 3, we estimate that the lowest number of hydroxyl groups in

TABLE 2: Product Classification According to Solubility Tests, Number of Hydroxyl Groups (MS and FTIR), and Polarity (TLC)

		MALDI-MS $C_{60}(OH)_n$			
		DHB	9-nitroanthraceno	FTIR	TLC[a]
soluble in H_2O, acetone, DMSO, DMF	insoluble in CH_3OH	commercial ($n = 7$)	O17 ($12 < n < 16$)	O17	O17
			80-10-L ($12 < n < 16$)	80-10-L	80-10-L
insoluble in H_2O	soluble in CH_3OH, DMSO; low solubility in acetone and benzene	80-10 ($n =$)	80-10 ($n = 9$)	80-10[b]	80-10
		25-10-Tb ($n =$)	25-10-Tb ($n = 8$)	25-10-Tb[b]	
insoluble in H_2O	insoluble in acetone; low solubility in CH_3OH, soluble in benzene	25-10-1 ($n =$)	25-10-1 ($n = 5$)	25-10-Ta[b]	25-10-1
		25-10-Ta ($n = 1$)	25-10-Ta ($n = 4$)	25-10-1[b]	

[a] From high to low polarity. [b] Fullerene is an important component in 25-10-1 and 25-10-Ta; fullerene is a minor contaminant in 80-10 and 25-10-Tb.

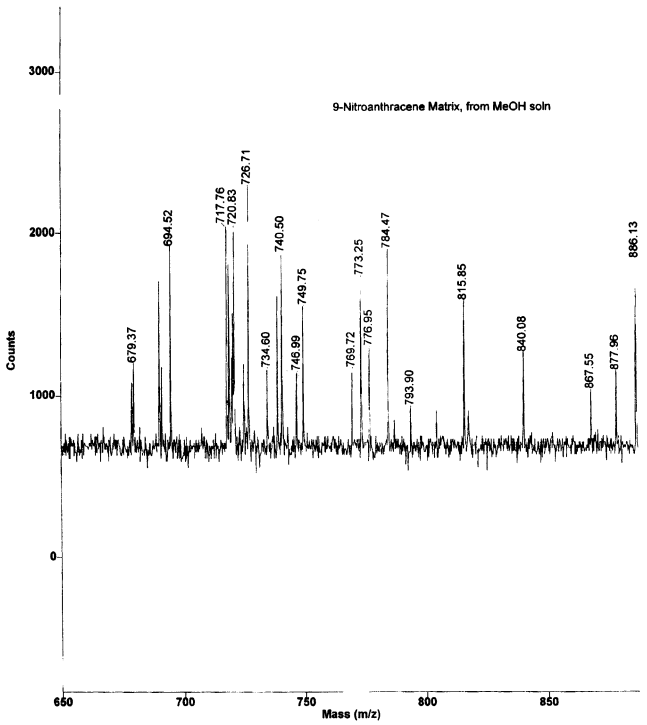

Figure 3. Mass spectrum of the 80-10 fraction used for monolayer formation using the MALDI technique with 9-nitroanthracene (NA) as matrix material.

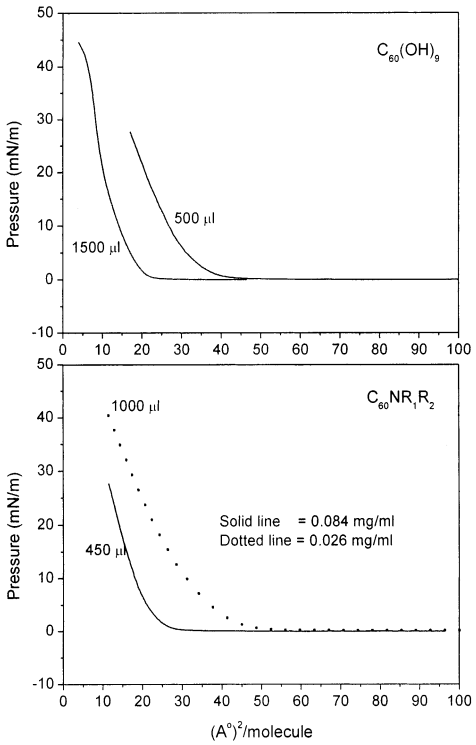

Figure 4. Surface pressure−area ($\pi-A$) isotherms: (a, top) product 80-10; (b, bottom) fulleropyrrolidine derivative.

this product fraction is ∼9. An upper limit for hydroxylation can be set on the basis of the work of Chiang et al.,[23] which reported slight water solubility for the dodecahydroxylated fullerene. Surface pressure−area ($\pi-A$) isotherms are shown in Figure 4a; the curves correspond to aliquots of different volumes. The molecular area A_0 (extrapolated to zero film pressure, $\pi = 0$) is half of the theoretical value (93 Å^2/molecule) or the experimentally determined value (96 Å^2/molecule) of pure C_{60}.[26,27] This suggests the formation of clusters instead of true monolayers, explaining the smaller A_0 at higher concentration (volume) of the deposited sample. The large volumes reported in the figure were necessary in order to get a significant surface pressure before the barriers were completely closed. The tendency of fullerene derivatives to form aggregates is also observed in the compound depicted in Figure 4b, where the group attached is characterized by its closed structure and by the presence of highly hydrophobic moieties (methyl and phenyl groups). In both compounds (Figure 4a and b), the films formed at the air/water interface were stable and did not show any noticeable area loss at a constant pressure of 20 mN/m.

The stable Langmuir films of both fullerene derivatives were transferred at 20 mN/m by the LB technique at a dipping speed < 3.5 mm/min. Higher transfer ratios (TR) were obtained during the upstroke in both compounds. The downstroke transfer ratio was significantly smaller in the substituted fulleropyrrolidine derivative. For optical and electrical characterization, two layers of fullerenol were deposited on glass substrates (TR = 85%$_{up}$, 7%$_{down}$, 71%$_{up}$) and on PANI/ITO substrates (TR = 96%$_{up}$, 45%$_{down}$, 100%$_{up}$). The lower transfer ratio of the more hydrophobic fulleropyrrolidine derivative required more depositions, two layers on glass substrates (TR = 50%$_{up}$, 0%$_{down}$, 33%$_{up}$) and four layers on PANI/ITO substrates (13%$_{up}$, 0%$_{down}$, 32%$_{up}$, 0%$_{down}$, 47%$_{up}$, 0%$_{down}$, 38%$_{up}$). The hydrophilic nature of the substrates explains the superior results in terms of surface coverage for the hydroxylated C_{60}. Furthermore, the large difference between the up and down transfer ratio indicates a LB film organization such as *substrate*$-(D-C_{60}-D-C_{60}-)_n$, where D stands for the specific derivative. This also suggests the large anisotropy of the hydroxylated fullerene, in contrast to the randomly bounded hydroxy groups reported by Chiang et al. The conditions used in two-phase catalysis for low levels of hydroxylation could force the reaction to take place mainly at the aqueous/solvent interface, hence promoting the formation of hydroxy groups clustered on one side of the cage. An alternative explanation might be that cluster formation minimizes the cage surface energy. Recent theoretical work (to be submitted), using a hybrid approach to calculate the structure and electronic properties of $C_{60}(OH)_n$, indicates that, up to $n =$

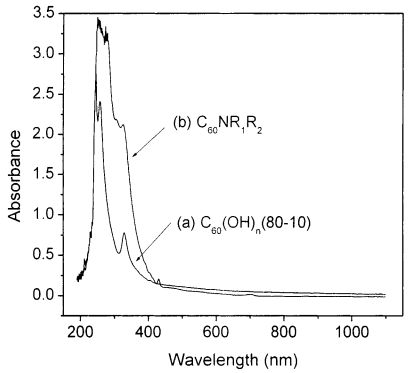

Figure 5. Optical absorption spectra of the solutions used for monolayer formation: (a) $C_{60}(OH)_9$ (fraction 80-10) in 2 mL of DMSO/23 mL of $CHCl_3$, $\sim 6 \times 10^{-5}$ M; (b) $C_{60}NR_1R_2$ in 25 mL of $CHCl_3$, $\sim 1 \times 10^{-4}$ M.

7, the OH groups like to bond forming a cluster on the C_{60} cage. The authors used a semiempirical modified neglect diatomic overlap (MNDO) calculation to determine the structure of the complex closest to the optimum, and density functional theory for energy minimization of the structures obtained. Previous theoretical work by Slanina et al.[26] also predicted a low symmetry molecule due to nonbonding interactions.

We must emphasize that although monomolecular layers of fullerenes and fullerene derivatives have been obtained by several groups, true monolayer deposition has been seen rarely.[27,28] C_{60} layers tend to cluster and form uneven films when transferred onto solid substrates.[29,30] In our films, the roughness of the polymeric matrix is another factor that makes it difficult to produce uniform films. It might explain the 45% transfer ratio of the fullerenol layer on PANI during the downstroke.

Optical and Electrical Characterization of LB Films. Figure 5 shows the optical absorption spectra of the solutions used for monolayer formation: (a) $C_{60}(OH)_9$ (fraction 80-10) in 2 mL of DMSO/23 mL of $CHCl_3$, $\sim 6 \times 10^{-5}$ M; (b) $C_{60}NR_1R_2$ in 25 mL of $CHCl_3$, $\sim 1 \times 10^{-4}$ M. The significant absorption maxima of fullerenol are at 246, 258, 330, and 405 nm, and the spectrum closely resembles that of monomer C_{60} with bands at 258 and 328 nm, a spike at 405 nm, and only a very weak absorption above it.[31] On the other hand, the spectrum of $C_{60}NR_1R_2$ shows significant maxima at 254, 278, 328, and 431 nm, and it resembles the one reported for substituted fulleropyrrolidine derivatives (280 and 432 nm).[32] From these data it is clear that aggregation does not occur in any of the working solutions and that true monomer solutions were used in monolayer formation.

The optical transmittance spectra of the two-layer LB films of fullerenol deposited on glass and PANI/ITO substrates are shown in Figure 6. From the curve of the LB film deposited on glass (labeled $C_{60}(OH)_n$80-10), no absorption is observed in the visible region and the onset corresponds to the absorption of the substrate. More information is obtained from the curve describing the LB film deposited on the PANI(ES) film (the semiconductor state of polyaniline). Here, the specimen labeled $C_{60}(OH)_n$80-10/PANI shows a spectrum with close resemblance to the spectrum of PANI(EB) (the insulate state of polyaniline), indicating the deprotonation of PANI(ES) by fullerenol. On the other hand, the four-layer LB film of the substituted fulleropyrrolidine derivative (labeled $C_{60}NR_1R_2$) deposited on the semiconductor polyaniline film (Figure 7) shows maximum transmittance bands of both the semiconductor PANI(ES) (around 550 nm) and the insulator PANI(EB) (around 750 nm). This might be interpreted as a partial deprotonation of the PANI

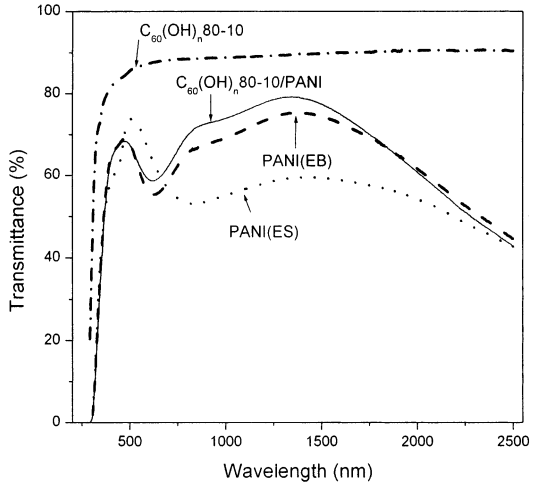

Figure 6. Optical transmittance spectra of fullerenol LB films deposited on glass and PANI/ITO substrates. The spectra of PANI substrates in their conducting (ES) and insulating (EB) forms are also shown.

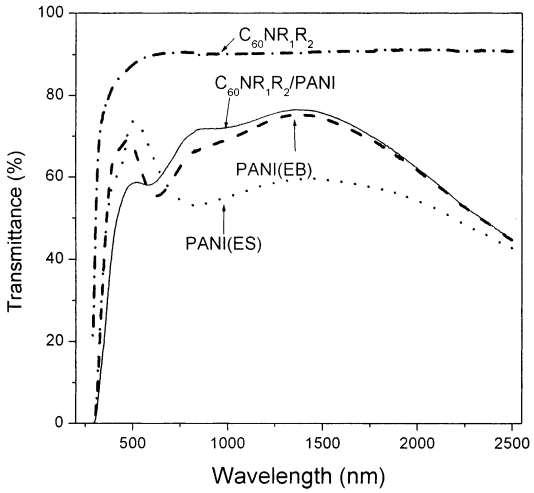

Figure 7. Optical transmittance spectra of substituted fulleropyrrolidine derivative LB films deposited on glass and PANI/ITO substrates. The spectra of PANI substrates in their conducting (ES) and insulating (EB) forms are also shown.

by the fulleropyrrolidine. A red-shift on the onset of absorption of the double film $C_{60}NR_1R_2$/PANI is another difference between the curves of fullerenol LB films, and the semiconducting and insulating PANI, suggesting the interaction of the functional groups. We must emphasize that deprotonation of PANI by these fullerene derivatives was not expected in our work. Reports indicated that the interaction of fullerene with polyaniline causes its oxidation upon photoactivation,[33,34] improving hole-based conductivity in reduced PANI (leucoemeraldine). In our work, the PANI used as a substrate was already oxidized and protonated to provide maximum conductivity.

With respect to the electrical properties of the two-layer LB films deposited on glass, the observed transfer ratios of both compounds suggest higher connectivity on the fullerenol LB film than on the $C_{60}NR_1R_2$ LB film. This agrees with the measured square resistance, which is a factor of 3 lower in the fullerenol film ($R_\square(C_{60}(OH)_n80\text{-}10) = 1.2 \times 10^{13}\ \Omega$; $R_\square(C_{60}NR_1R_2) = 3.5 \times 10^{13}\ \Omega$). Taking into account the number of films transferred and the measured A_0, we estimate as 5 nm the thickness of the LB films deposited on glass. That gives conductivity values of $1.7 \times 10^{-7}\ \Omega^{-1}\ cm^{-1}$ for fullerenol and $5.7 \times 10^{-8}\ \Omega^{-1}\ cm^{-1}$ for the substituted fulleropyrrolidine,

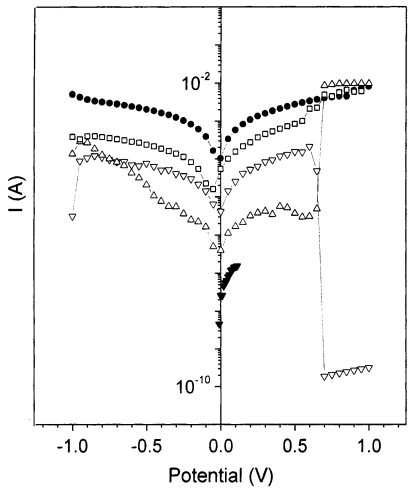

Figure 8. *I*−*V* curves of the two-layer LB fullerenol film deposited on PANI/ITO taken at different regions of the LB film, with various delay times between measurements. Curves labeled ▽ and ▼ were taken at the same point, in that order.

which are close to the highest conductivity value reported for polymeric C_{60} ($\sigma = 10^{-6}$ to 10^{-12} Ω^{-1} cm^{-1}).[35] The electronic conductivities reported for fullerenol LB films strongly disagree with the 10^{-14} Ω^{-1} cm^{-1} reported for $C_{60}(OH)_{12}$,[19] suggesting a substantial improvement due to the more organized structure of LB films.

The estimate of the fullerenol LB film thickness is based upon the assumption of similar molecular areas in fullerenol and C_{60} (96 Å^2/molecule). This gives a molecular diameter (layer thickness) of ∼11 Å, which is not much different from the 12 ± 2 Å reported by Chiang et al. for monolayers of $C_{60}(OH)_{12}$.[15] Due to the large anisotropy of the fullerenol molecule studied here, we do not expect the hydroxyl groups to contribute to the effective diameter significantly, since they are mostly in contact with the water subphase. In the case of the randomly distributed hydroxyl groups, the OH's placed around the symmetry axis of the molecule parallel to the water surface could increase the effective diameter up to 15 Å.

The optoelectronic properties of the LB films were investigated, and no significant photocurrent was obtained under white light illumination, in agreement with the UV−vis data. Even so, dark measurements provided some information about the characteristics of the conductive polymer/fullerenol junction. Figure 8 shows the *I*−*V* curve of the two-layer LB fullerenol film deposited on PANI/ITO. The various curves were taken at different regions of the LB film with various delayed times between measurements, while the curves labeled 1 and 2 were taken at the same point, in that order. The transients on those curves indicate nonuniform films. For instance, in some regions a particular voltage increases the resistivity of the film, while in other regions the same voltage increases its conductivity. Films degradation does not occur, since some reversibility is observed. Curve 1, for example, has a large drop in conductivity at around 0.7 V but recovers once the voltage is decreased (curve 2). The strong interaction between fullerenol and PANI, inferred from UV−vis studies (Figure 6), and the reported proton conductivity of fullerenol[19] might account for the unpredictable response at large bias. To minimize possible sources of error, the *I*−*V* curves of both LB films were plotted from discrete measurements; that is, the voltage was sustained for 300 s and the average current measured. Figure 9 shows the *I*−*V* curves for fullerenol (a) and the substituted fulleropyrrolidine (b). The larger asymmetry of the fullerenol LB film indicates the higher

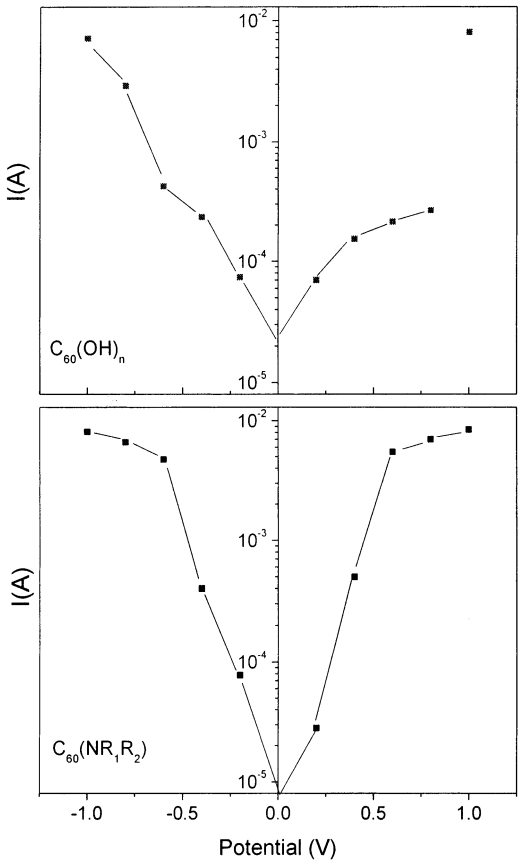

Figure 9. Comparison of the *I*−*V* curves of (a) the fullerenol LB film and (b) the substituted fulleropyrrolidine LB film.

rectifying nature of the PANI/fullerenol junction, expected in donor/acceptor interfaces, while no rectifying character is observed in the $C_{60}NR_1R_2$/PANI junction.

The comparison of *I*−*V* curves of ITO/PANI/(commercial fullerenol)$_{drop/evap}$ versus ITO/PANI/(fullerenol)$_{LB}$ shows higher current and rectifying character in the latter, confirming the hypothesis that the electrical properties of the conductive polymer/fullerenol junction improve as the number of hydroxyl groups decreases on the C_{60} cage and when organized structures are formed at the interface. The data also show the importance of minimizing the amount of basic groups in the fullerene cage, since they deprotonate PANI, compromising the beneficial effects expected from a more organized interface. Incomplete hydroxylation was observed in the fraction used for monolayer formation, and this could cause the deprotonation of PANI. Still, the reported proton conductivity of fullerenol suggests that deprotonation of PANI will occur even in completely hydroxylated molecules. Therefore, we expect the junctions of fullerenol with polyaniline films in its reduced (leucoemeraldine) or deprotonated (emeraldine base) states to have a more stable response, showing more clearly the advantages expected in an organized donor/acceptor interface.

Conclusions

We report the synthesis of hydroxylated fullerene derivatives, prepared to improve the ordering of Langmuir films at the air/water interface as well as the electrical properties of LB films transferred to glass and semiconducting polyaniline substrates. The different transfer ratios of LB films during up and down strokes suggest a large anisotropy on the $C_{60}(OH)_n$ molecule. This anisotropy might be due to the fact that, under the conditions of low hydroxylation in two-phase catalysis, the

reaction takes place mainly at the aqueous/organic interface, leading to clustering of the OH groups. Another possible explanation relies on theoretical calculations that indicate that at low levels of hydroxylation the clustering lowers the surface energy of the substituted fullerene. The electrical conductivities of fullerenol LB films deposited on glass are equivalent to that of highly conductive polymeric C_{60} and various orders of magnitude higher than that reported for disordered fullerenol pellets. Total or partial deprotonation of semiconducting polyaniline films is observed in both fullerenol and substituted fulleropyrrolidine derivatives. It might be a consequence of the combined effect of the strong electronegativity of the C_{60} cage and the large proton mobility of these films. The $I-V$ curves of fullerene derivatives/PANI indicate some rectifying character at the fullerenol/PANI junction, while no rectification is observed on the substituted fulleropyrrolidine/PANI double layer film. The transients observed at the fullerenol/PANI junctions are consistent with the reported proton conductivity of fullerenol.

Acknowledgment. The authors are grateful to F. Wudl and R. Helgenson for assistance with the synthesis of fullerenol and to C.M. Knobler and K. Hisada for assistance with LB films preparation. We acknowledge the financial support of UCMEXUS-CONACyT.

References and Notes

(1) Friedman, S. H.; Ganapathi, P. S.; Rubin, Y.; Kenyon, G. L. *J. Med. Chem.* **1998**, *41*, 2442.

(2) Chen, H. C.; Yu, C.; Veng, T. H.; Chen, S.; Huang, K. J.; Chiang, L. Y. *Toxicol. Pathol.* **1998**, *26*, 143.

(3) Miyata, N.; Yamakoshi, Y. In *Fullerenes: Recent Advances in the Chemistry and Physics of Fullerenes and Related Materials*; Kadish, K. M., Ruoff, R. S., Eds.; The Electrochemical Society: Pennington, NJ, 1995; Vol. 5, p 345.

(4) Chiang, L. Y.; Upasani, R. B.; Swirczewsky, J. W.; Soled, S. *J. Am. Chem. Soc.* **1992**, *114*, 10154.

(5) Chiang, L. Y.; Swirczewsky, J. W.; Hsu, C. S.; Chowdhury, S. K.; Cameron, S.; Creegan, K. *J. Chem. Soc., Chem. Commun.* **1992**, 1791.

(6) Chiang, L. Y.; Upasani, R. B.; Swirczewsky, J. W.; Soled, S. *J. Am. Chem. Soc.* **1993**, *115*, 5453.

(7) Chiang, L. Y.; Wang, L. Y.; Swirczewski, J. W. *J. Org. Chem.* **1994**, *59*, 3960.

(8) Chiang, L. Y.; Bhonsle, J. B.; Wang, L. Y.; Shu, S. F.; Chang, T. M.; Hwu, J. R. *Tetrahedron* **1996**, *52*, 4963.

(9) Chen, B. H.; Huang, J. P.; Wang, L. Y.; Shiea, J.; Chen, T. L.; Chiang, L. Y. *J. Chem. Soc., Perkin Trans.* **1998,** *1*, 1171.

(10) Jin, H.; Chen, W. Q.; Tang, X. W.; Chiang, L. Y.; Yang, C. Y.; Schloss, J. V.; Wu, J. Y. *J. Neurosci. Res.* **2000,** *62*, 600.

(11) Lai, H. S.; Chen, W. J.; Chiang, L. Y. *World J. Surg.* **2000**, *24*, 450.

(12) Huang H. M.; Ou, H. C.; Hsieh, S. J.; Chiang, L. Y. *Life Sci.* **2000**, *66*, 1525.

(13) Lai Y. L.; Chiou, W. Y.; Lu, F. J.; Chiang, L. Y. *Br. J. Pharmacol.* **1999**, *126*, 778.

(14) Lu, L. H.; Lee, Y. I.; Chen, H. W.; Chiang, L. Y.; Huang, H. C. *Br. J. Pharmacol.* **1998**, *123*, 1097.

(15) Ueng, T. H.; Kang, J. J.; Wang, H. W.; Cheng, Y. W.; Chiang, L. Y. *Toxicol. Lett.* **1997**, *93*, 29.

(16) Lai, Y. L.; Chiang, L. Y. *J. Auton. Pharmacol.* **1997**, *17*, 229.

(17) Tsai, M. C.; Chen, Y. H.; Chiang, L. Y. *J. Pharm. Pharmacol.* **1997**, *49*, 438.

(18) Kyokane, J.; Tokugi, K.; Uranishi, D.; Miyata, M.; Ueda, T.; Yoshino, K. *Synth. Met.* **2001**, *121*, 1129.

(19) Hinokuma, K.; Ata, M. *Chem. Phys. Lett.* **2001**, *341*, 442.

(20) Sariciftci, N. S.; Smilowitz, L.; Heeger, A. J.; Wudl, F. *Science* **1992**, *258*, 1474.

(21) Wang, P.; Metzger, R. M.; Chen, B. *Thin Solid Films* **1998,** *327*−*329*, 96.

(22) Wang, S.; Leblanc, R. M.; Arias, F.; Echegoyen, L. *Thin Solid Films* **1998**, *327*−*329*, 141.

(23) Liu, W. J.; Jeng, U.; Lin, T. L.; Lai, S. H.; Shih, M. C.; Tsao, C. S.; Wang, L. Y.; Chiang, L. Y.; Sung, L. P. *Physica B* **2000**, *283*, 49.

(24) Li, J.; Takeuchi, A.; Ozawa, M.; Li, X.; Saigo, K.; Kitazawa, K. *J. Chem. Soc., Chem. Commun.* **1993**, 1784.

(25) Kinoshita, K. *Carbon. Electrochemical and Physicochemical Properties*; Wiley-Interscience Publication; John Wiley & Sons: New York, 1988.

(26) Slanina, Z.; Zhao, X.; Chiang, L. Y.; Osawa, E. *Int. J. Quantum Chem.* **1999**, *74*, 343.

(27) Mirkin, C. A.; Caldwell, W. B. *Tetrahedron* **1996**, *52*, 5113.

(28) Castillo, R.; Ramos, S.; Ruiz-Garcia, J. *J. Phys. Chem.* **1996**, *100*, 15235.

(29) Wang, P.; Shamsuzoha, M.; Wu, X.; Lee, W.; Metzger, R. M. *J. Phys. Chem.* **1992**, *96*, 9027.

(30) Williams, G.; Pearson, G.; Bryce, M. R.; Petty, M. C. *Thin Solid Films* **1992**, *209*, 150.

(31) Yamakoshi, Y. N.; Yagami, T.; Fukuhara, K.; Sueyoshi, S.; Miyata, N. *J. Chem. Soc., Chem. Commun.* **1994**, 517.

(32) Guo, Z.; Li, Y.; Bai, F.; Yan, J.; Ge, Z.; Zhu, D.; Si, J.; Ye, P.; Wang, L.; Li, T. *J. Phys. Chem. Solids* **2000**, *61*, 1089.

(33) Anantharaj, V.; Patil, S. V.; Canteenwala, T.; Wang, L. Y.; Chiang, L. Y. *Synth. Met.* **2001**, *121*, 1123.

(34) Langer, J. L.; Framski, G.; Golezak, S.; Gibinski, T. *Synth. Met.* **2001**, *119*, 359.

(35) Makarova, T. L.; Sundqvist, B.; Scharff, P.; Gaevski, M. E.; Olsson, E.; Davydov, V. A.; Rakhmanina, A. V.; Kashevarova, L. S. *Carbon* **2001**, *39*, 2203.